J Appl Electrochem (2008) 38:1005–1010
DOI 10.1007/s10800-008-9526-2

ORIGINAL PAPER

FEM model of the ohmic resistance of IP-SOFCs

Laura Repetto · Paola Costamagna

Received: 15 September 2007 / Revised: 14 February 2008 / Accepted: 19 February 2008 / Published online: 7 March 2008

Abstract In the present work, the ohmic resistance of an integrated planar-SOFC (IP-SOFC) has been evaluated by developing a model whose equations have been solved numerically through an FEM method. The model allows to estimate the distribution of voltage and current density in the cell. A comparison between simulated and experimental data of area specific resistance is reported, which shows satisfactory agreement. The mathematical model has also been used to carry out some parametric studies for optimisation purposes. Indeed, a reduction in cell pitch length and an increase in electrode thickness are predicted to lead to a reduction in ohmic losses in IP-SOFCs.

Keywords Solid oxide fuel cell · Integrated planar solid oxide fuel cell · Ohmic resistance · Partial differential equation · Finite elements method

Nomenclature

ASR_O	Ohmic area specific resistance (Ω cm^2)
V	Voltage (V)
x	Co-ordinate (cm)
y	Co-ordinate (cm)
Greek letters	
Ω	Domain
Γ	Interface
σ	Conductivity (Ω^{-1} cm^{-1})
Subscripts	
i	Cell component
1	Anode
2	Electrolyte
3	Cathode
4	Interconnect
5	Cathode

L. Repetto · P. Costamagna (✉)
DICHEP, University of Genoa, Via all'Opera Pia 15, 16145 Genoa, Italy
e-mail: paola.costamagna@unige.it

1 Introduction

The main types of SOFC can be classified as planar/monolithic (a monolith being formed of a number of planar cells stacked together) [1] and tubular [2, 3]. The planar cell design offers high power density and cheap manufacturing costs, but unfortunately in this geometry, at the high operating temperature (about 1,000 °C), the mismatch of thermal expansion of the various components can cause cracking of the structure, with consequent loss of performance. In the tubular cell design, the cell is tube-shaped and only one end of the tube is mechanically constrained; thus, the structure is free to expand at high temperatures and mechanical stresses are minimised, preventing cracking of the cell components. Unfortunately, the manufacturing costs are high, because of the necessity to keep the diameter small (about 2 cm) in order to reduce current paths and improve cell efficiency. At present, various alternative cell designs are under development to avoid difficulties relating to mechanical stress and reduce the high manufacturing costs. One of the possible alternative cell designs is the IP-SOFC [4] developed by Rolls-Royce Fuel Cell Systems Ltd (RRFCS), which is substantially a cross between tubular and planar configurations.

Under typical operating conditions a single IP-SOFC produces less than 1 V. To obtain high voltage and power, a number of single cells are electrically connected in series using interconnect materials. A section of an IP-SOFC and the sequence of the various components, including the interconnects, is shown in Fig. 1, where the chemical and

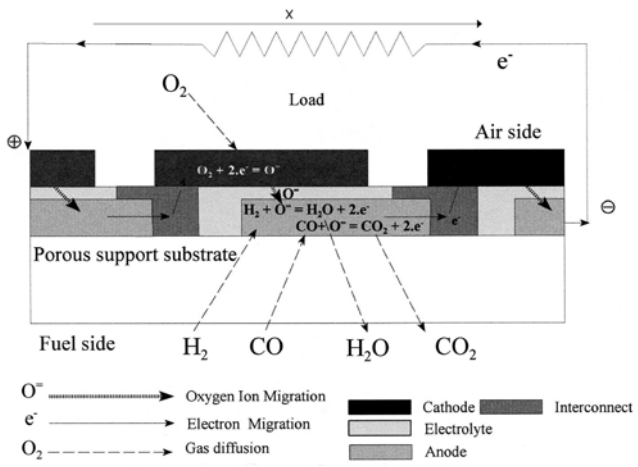

Fig. 1 Schematic drawing of a section of the IP-SOFC geometry

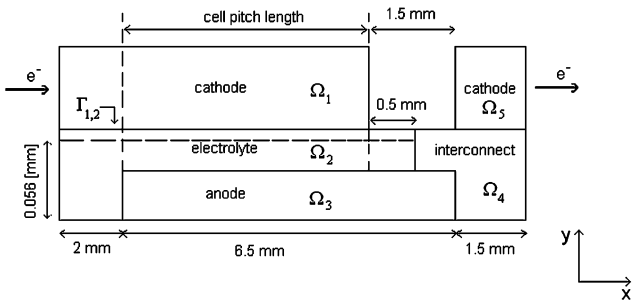

Fig. 2 Repetitive unit of a section of the IP-SOFC geometry

electrochemical reactions along with the current paths through each cell are shown.

Ohmic losses account for a large part of the overall losses occurring in SOFCs, and significantly affect cell performance. Thus, a theoretical estimate of the ohmic resistance is important, especially in view of optimisation. Nevertheless, in the case of complex cell geometries, a detailed evaluation of the ohmic losses is not a simple task because numerical solution of a PDE system is necessary. Among numerical methods, FEMs [5] are usually preferred because of their high flexibility and accuracy. Their basic concept consists first of establishing a "weak" variational formulation of the mathematical problem; the second step is to introduce the concept of shape functions that are defined into small subregions of the domain (that altogether form the so-called mesh). Finally, the variational equations are discretised and form a linear system where the unknowns are the coefficients of the linear combination. Since the implementation of a code based on FEM and, in particular, the mesh building is not a simple task, commercial software packages that allow the application without implementing an "in-house" code are often used. In this work, the commercial package Comsol Multiphysics© has been used to evaluate the ohmic resistance of an IP-SOFC.

In other work [6], a detailed evaluation of the ohmic resistance of a simplified cell geometry has been carried out. In particular, a comparison between the results obtained with Comsol Multiphysics© and a code developed "in house" based on finite difference method (FDM) [7] was made.

The aim of the present work is to establish a mathematical model to estimate the ohmic resistance of the IP-SOFC and validate the results obtained through comparison with experimental data provided by RRFCS.

RRFCS has developed several IP-SOFCs with different designs and geometrical data. The design presented in this paper is not exactly that selected for the market, which, for obvious confidentiality reasons, cannot be published. However, the design presented in this paper is similar to that for the market, and has been investigated from both the experimental and the theoretical point of view. Thus, the results presented have interest for both scientific and application purposes.

2 Theoretical model

Figure 2 shows a schematic drawing of the repetitive unit of the IP-SOFC along with some geometrical data. The simulation results reported in this paper have been obtained considering a 10 μm-thick electrolyte, 50 μm-thick electrodes and the following material properties at 900 °C: cathode conductivity 128.7 S cm^{-1}; electrolyte conductivity 0.06111 S cm^{-1}; anode conductivity 304 S cm^{-1}. The electrodes are electronic conductors and the electrolyte is an ionic conductor. An IP-SOFC operating with a current density of 0.32 A cm^{-2} is considered.

The results reported in this paper concern only the calculation of ohmic losses, while the electrochemical reactions at the cathode–electrolyte and electrolyte–anode interfaces are not taken into account.

2.1 Mathematical formulation of the problem

The physical problem involves calculation of distributions of potential and electrical current density in solid, homogeneous and isotropic ohmic conductors. In every layer of the IP-SOFC geometry (Fig. 2), the physical phenomena are totally described through the equation of current continuity. Figure 2 shows the mathematical notation; in particular, we denoted:

$$\Omega = \Omega_1 \cup \Omega_2 \cup \Omega_3 \cup \Omega_4 \cup \Omega_5;$$

In the case of the problem analysed in this paper, the equation satisfied by potential into $\Omega_i (\forall\, i = 1, 2, 3, 4, 5)$ can be simplified in the Laplace equation:

$$\frac{\partial^2 V_i}{\partial x^2}(x) + \frac{\partial^2 V_i}{\partial y^2}(x) = 0 \quad (1)$$

$\forall x \in \Omega_i$.

Along the interior boundaries of the IP-SOFC geometry (Fig. 2), except for the contact line between the electrolyte and interconnect material where the electrical insulation is imposed, potentials connect with continuity and no electrical charges are accumulated on them. The last assumption can be expressed by stipulating that the normal components of the electrical current are continuous across the interior boundaries. For example, considering the subdomains Ω_1 and Ω_2 (Fig. 2), with electrical conductivities σ_1 and σ_2 respectively, in contact with each other through the line $\Gamma_{1,2}$, then the condition over interface can be expressed as follows:

$$V_{1|\Gamma_{1,2}} = V_{2|\Gamma_{1,2}} \quad (2)$$

$$\sigma_1 \frac{\partial V_1}{\partial y}(x) - \sigma_2 \frac{\partial V_2}{\partial y}(x) = 0 \quad (3)$$

Finally, on the borderlines where the current enters and exits (Fig. 2), the value of the current density is known, whereas over the remaining external boundaries, electrical insulation is imposed.

Further details about the model equations can be found in [6].

2.2 Comsol Multiphysics simulation

Comsol Multiphysics is a modelling package for the simulation of physical processes which are described by PDEs. Further details about the potentialities of this tool can be found in the software manuals [8, 9].

In the simulation described in this paper, the *Electromagnetics Application Modes* and in particular the *Conductive Media DC Application Mode*, included in version 3.3 of the software, have been used [8, 9]. The automatic mesh generator and default solver have been applied. In particular a triangular mesh with Lagrange-quadratic elements has been considered and the option 'Adaptive Mesh Refinement' has been applied. With this option, the software automatically identifies the portions of the geometry where mesh refinement is necessary and increases mesh refinement in these portions, which are located at the two ends of the active cell region. With this procedure, the number of elements of the mesh is about 70,000 and the number of degrees of freedom is about 140,000. The results reported have been obtained with the mesh described above. To check the accuracy of the solution, mesh grid sensitivity has been run. The results change only very slightly with increasing number of elements from 8,000 to 270,000. For example, we have checked the results obtained for the overall ohmic resistance of the cell (expressed in terms of Ohmic Area Specific Resistance, ASR_O) by varying the number of elements of the mesh. For example, when the number of mesh elements is 8.000 and 270.000 the ASR_O is respectively 0.02% and less than 0.003% different from the reference value obtained with the reference mesh element of 70,000.

3 Results

The colour map of the voltage is shown in Fig. 3. The potential is higher where the current enters the structure, on the left-hand side, while it is lower where the current exits the cell, on the right-hand side.

Figure 4a shows the current lines. Figure 4b zooms the contact region between the electrolyte and the interconnect material. Figure 4a shows two features of the current lines: (i) that they cross the electrolyte perfectly cross-plane, which is due to the fact that the electrolyte has by far the highest resistance among all the materials employed, and (ii) that the electrical current flows through the electrodes mainly in the in-plane direction, expanding almost uniformly across the electrode thickness. This is further demonstrated by Fig. 5, which displays the values of the *x*-component of the current density vector along a vertical line located at a length co-ordinate of 0.3 cm.

Figure 4b shows that most of the electrical current flowing through the anode crosses the interconnection very close to the contact region between the electrolyte and the interconnect material. This is reasonable because the electrical conductivity of the interconnection is far higher than that of the anode.

In Fig. 6 the values of the current density norm along the horizontal line situated in the electrolyte at *y*-coordinate 0.0056 cm (see Fig. 2) are plotted versus cell length. With this choice of geometry and conductivities, the distribution of the current density norm is not uniform in the active part of the cell. In particular, it is interesting to note that the

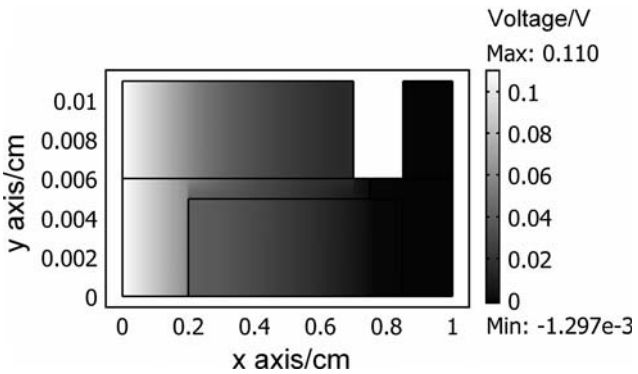

Fig. 3 Simulation results at 900 °C: colour map of the voltage

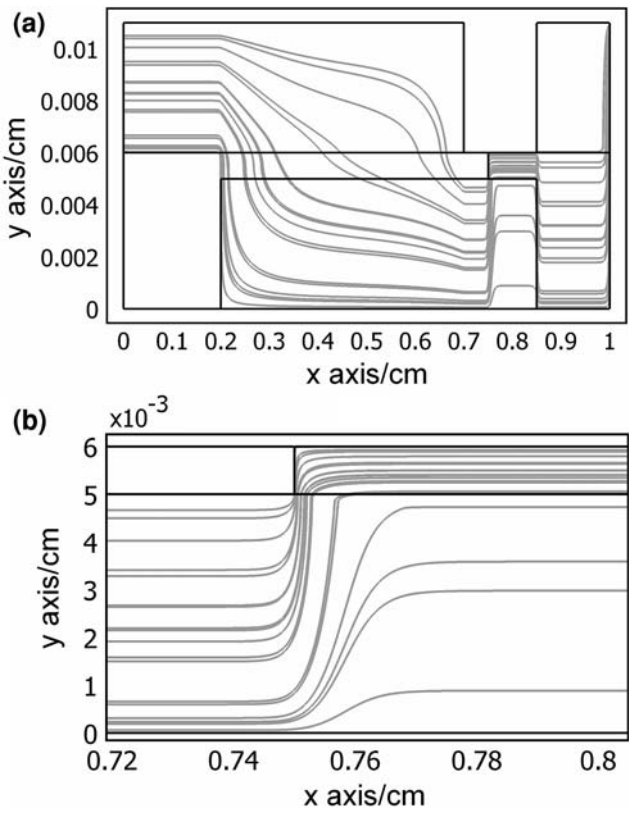

Fig. 4 Simulation results at 900 °C. (**a**) Current lines; (**b**) Current lines: enlargement of the contact region between the electrolyte and the interconnect material

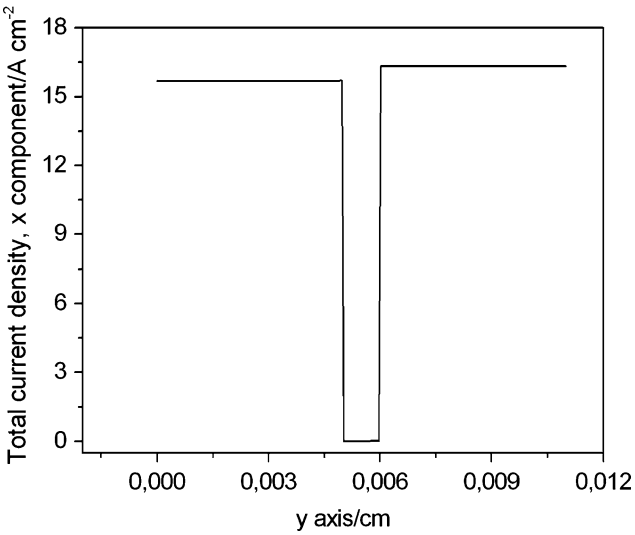

Fig. 5 Simulation results at 900 °C: values of the x-component of the current density vector along a vertical line located at a length coordinate $x = 0.3$ cm

current crossing the electrolyte is almost zero in the region between 0.45 and 0.55 cm.

Finally, Fig. 7 shows a comparison between the values of the ASR_O obtained with Comsol Multiphysics and the

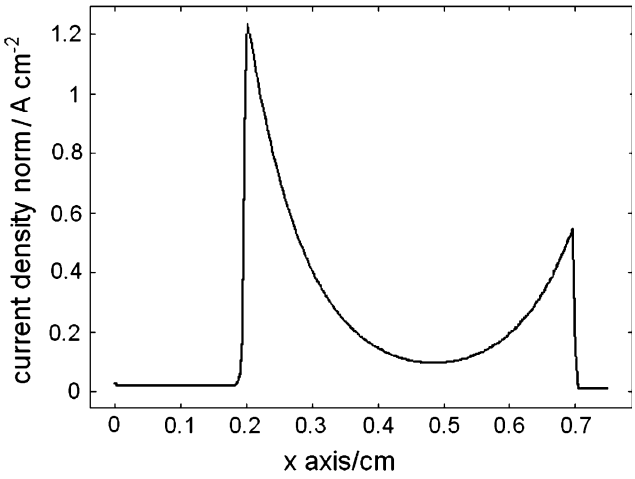

Fig. 6 Simulation results at 900 °C: norm of the current density vector along a horizontal line in the electrolyte (y-coordinate 0.0056 cm, please see Fig. 2)

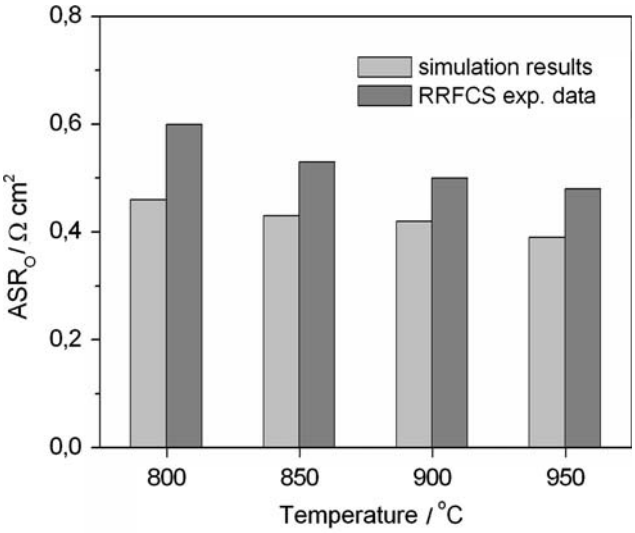

Fig. 7 ASR_O values: comparison between simulation results and experimental values

experimental data provided by RRFCS. The geometry used in both the experiments and the simulations is close to that discussed above. In Fig. 7, the simulation results are reported together with the experimental data obtained with the electrochemical impedance spectroscopy technique (EIS). The experimental values and simulation results have been obtained at various operating temperatures between 800 and 950 °C. The error in estimating the experimental values is about 24%, and this discrepancy can be explained considering that the simulation does not take contact resistance into account. The concept of contact resistance in fuel cells is discussed by many authors [e.g. 10], based on the idea that the adhesion among the different layers which compose a fuel cell is never ideal, leading to the

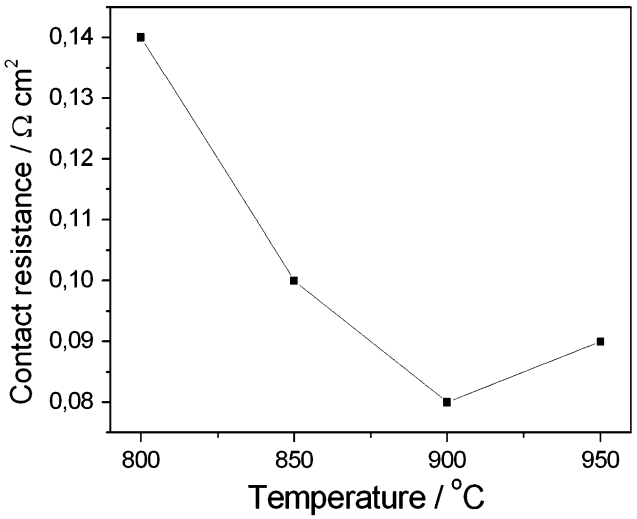

Fig. 8 Area specific contact resistance as a function of temperature

formation of bottlenecks through which the charge is forced to flow, causing voltage losses and thus an additional resistance. In order to have an approximated evaluation of contact resistances, simulation and experimental errors have been hypothesised to be negligible, and the difference between the experimental and the simulated values of the ohmic resistance have been attributed entirely to contact resistance. The results are reported in Fig. 8 as a function of temperature, displaying an average value of about 0.10 Ω cm^2 in the temperature range under consideration (800–950 °C).

4 Parametric studies and optimisation remarks

Optimisation of the IP-SOFC should be carried out through a complete simulation tool, also taking into account activation and concentration losses, as well as an evaluation of temperature and distribution of reactant concentration over a full size stack. However, some preliminary considerations about optimisation can be made on the basis of the model presented here, in particular concerning the effects that changes in geometry have on the ASR_O. In particular, the effects of changes in the cell pitch length (defined in Fig. 2) and electrode and electrolyte thickness are reported in Fig. 9. All the calculations have been carried out at 900 °C; the results are reported in terms of dimensionless ASR_O, defined as the ratio between the actual ASR_O and the value calculated with the reference geometrical data (Fig. 2) at 900 °C.

Figure 9a displays the variation of the dimensionless ASR_O as a function of the cell pitch length, and in particular the figure shows that the ASR_O decreases with decreasing cell pitch length. This is due to the fact that the voltage losses due to the in-plane path of the electrons in the electrodes is the main contribution to ohmic losses (being larger than the voltage losses caused by the flow of

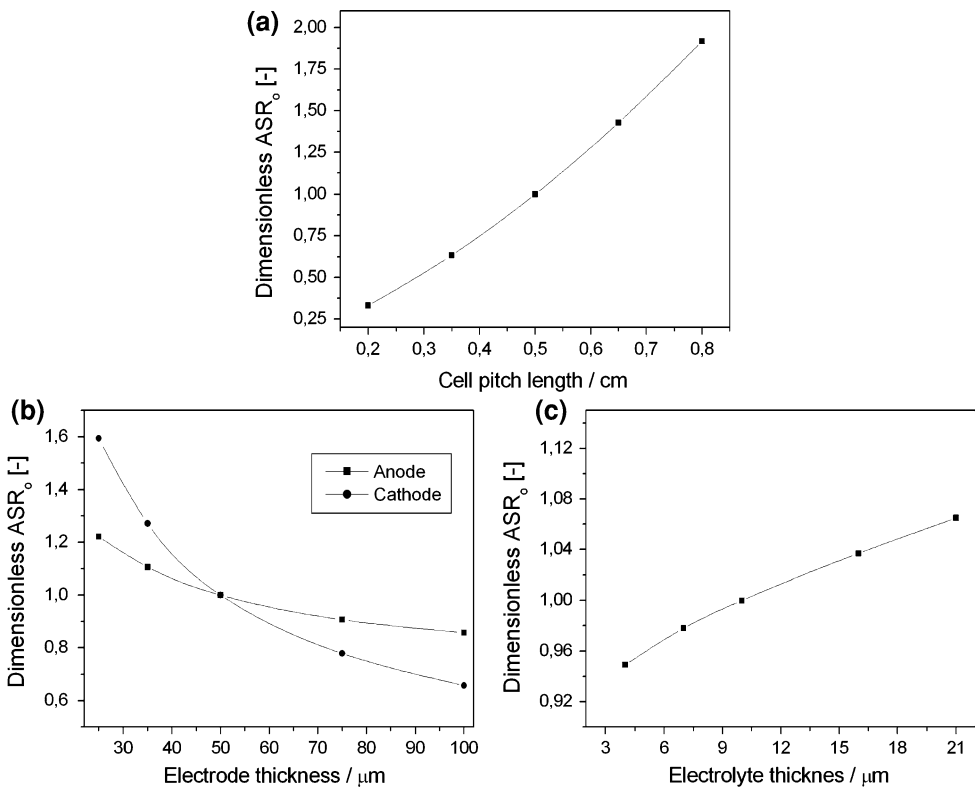

Fig. 9 ASR_O as a function of the cell pitch length (**a**), electrode thickness (**b**) and electrolyte thickness (**c**). Operating temperature: 900 °C. Symbols: simulated values. Lines: spline interpolations

oxygen ions through the electrolyte). Thus, by reducing the cell pitch length the in-plane path of the electrons in the electrodes is also reduced and, finally, this causes a reduction of the ASR_O.

Also the results reported in Fig. 9b are a consequence of the main contribution of electrode losses to the ASR_O. Indeed, Fig. 9b shows that an increase in electrode thickness causes a significant decrease in the ASR_O, due to the larger cross-section area available for flow of electrons in the electrodes, which leads to a reduction of the in-plane voltage losses. In Fig. 9b, results for electrodes larger than 100 μm are avoided since for such thicknesses concentration losses might play a significant role and change the results appreciably [11]. For electrodes thinner than 100 μm and considering the standard SOFC electrode porosities (about 30%), concentration losses usually are considered negligible due to the high operating temperatures. Figure 9b also shows that the decrease of ASR_O is more significant when changing the cathode rather than the anode thickness, due to the cathodic conductivity being lower than the anodic.

Finally, Fig. 9c shows that the ASR_O decreases only slightly when the electrolyte thickness is reduced. This is due, as remarked above, to the fact that voltage losses through the electrolyte are less significant than voltage losses in the electrodes.

The results discussed in this section give some hints about geometric optimisation. Indeed, a reduction in cell pitch length and an increase in electrode thickness are expected to lead to a reduction in ohmic losses in IP-SOFCs. Again, a complete model also including activation and concentration effects can give further interesting indications for optimisation.

5 Conclusions and future work

Modelling of the ohmic resistance of IP-SOFCs has been performed, and the simulation results have been compared with experimental data provided by RRFCS. The mathematical model has also been used to carry out some parametric studies useful for optimisation purposes. In future work, the numerical tool will be used as the basis for the development of a complete simulation tool, performing the simultaneous evaluation of ohmic, activation and concentration effects.

Acknowledgements The authors thank Rolls-Royce Fuel Cell Systems Ltd for financial support, and for supplying the experimental data. In particular, thanks go to Robert Collins of RRFCS for interesting discussions. The authors also acknowledge the British Council/CRUI project for funding an exchange of visits between RRFCS and the University of Genoa aimed at transferring the experimental data for model validation.

References

1. Tietz F, Buchkremer HP, Stöver D (2002) Solid State Ionics 152:373
2. Bessette NF, Wepfer WJ, Winnic J (1995) J Electrochem Soc 142:3792
3. Singhal SC (2000) Solid State Ionics 135:305
4. Gardner FJ, Day MJ, Brandon NP et al (2000) J Power Sources 86:122
5. Pepper DW, Hernrich JC (2006) The finite element method. Taylor & Francis Group, New York
6. Repetto L, Agnew G, Del Borghi A et al (2007) J Fuel Cell Sci Technol 4:413
7. Strikwerda JC (2004) Finite difference scheme and partial differential equations, 2nd edn. SIAM Publications, Cambridge
8. Comsol Multiphysics User's Guide Version 3.2 (2005) COMSOL AB, Stockholm
9. Comsol New Features Guide Version 3.3 (2006) COMSOL AB, Stockholm
10. Metzger P, Friedrich KA, Müller-Steinhagen H Schiller G (2006) Solid State Ionics 177:2045
11. Cannarozzo M, Grosso S, Agnew G et al (2007) J Fuel Cell Sci Technol 4:99